2023 62nd IEEE Conference on Decision and Control (CDC)
December 13-15, 2023. Marina Bay Sands, Singapore

Fractional-order position control for the fully-actuated Hexa-rotor: SITL simulations in the PX4 firmware

Andrés Montes de Oca[1], Alejandro Flores[1], Micky Rakotondrabe[2], *Member, IEEE*, and Gerardo Flores[1], *Member, IEEE*

***Abstract*— This paper presents a fractional-order controller for the fully-actuated Hexa-rotor under external disturbances applied to the position and attitude dynamics. We proved that the closed-loop system equilibrium point for the positioning subsystem is globally exponentially stable. Furthermore, the controller provides extraordinary robustness to the system when affected by exogenous and aggressive disturbances. The system's stability is also validated through MATLAB and software in the loop simulations. One of the paper's contributions, apart from the control design, is the implementation of the controller in the PX4 firmware, the most popular open-source autopilot code used worldwide for flying drones. The code is available for download and implemented in real drones. Finally, we have implemented the control algorithm in the PX4-firmware alongside a virtual environment in Gazebo and compared it with the standard PX4-firmware controller. The results considerably outperform the traditional PID controller programmed in the PX4 firmware.**

I. Introduction

In recent years, the research community has addressed the disturbance robustness problem in Unmanned Aerial Vehicles (UAVs) using robust control techniques such as sliding mode control and others [1], [2]. In particular, this kind of control has adopted the use of integer-order control approaches [3], [4]. However, since UAVs' attitude and position are coupled, and their dynamics are subjected to external disturbances, the interest in proposing robust controllers for fully actuated multi-rotors has emerged in the last few years. The fully-actuated multi-rotors can partially decouple the attitude and position dynamics. They can be more appropriate for solving special tasks such as agricultural harvesting [5], [6], or aerial manipulation [7].

A. State of the art

Standard fractional-order sliding mode controls (FOSMC) have been developed as in [8]–[12], for quadrotor UAVs considering external disturbances to achieve a more robust behavior. Then, [13], [14] propose similar approaches for FOSMCs based on the backstepping method. A variant of the FOSMC can be found in [15] through an event-trigger-based strategy. The PI control structure is also proposed in [16] with a fractional-order integral combined with sliding mode control. Furthermore, in [17], it is presented as a fractional-order PID controller, where derivative action proves to enhance the control response of the system. Similarly, [18] presents a fractional-order linear active disturbance rejection control scheme combining the advantages of the fractional-order PID with the linear active disturbance rejection control. Then, [19] proposes a fractional nonlinear control strategy based on the nested saturations to maintain the desired position and orientation in stationary flight and trajectory tracking tasks. The fractional-order control technique is not inherent to quadrotor UAVs, as it is also used in other vehicles, such as fixed-wing aircraft. For instance, [20], [21], present a Finite-time Fault-Tolerant Control using a fractional-order backstepping iterative design strategy for fixed-wing aircraft. According to state-of-the-art, the fractional-order controls for fully-actuated multi-rotor configurations is a new research topic, particularly when the control is coded or applied to an autopilot. With a lack of this kind of control applied to the fully actuated Hexa-rotor, we summarize recent works using other robust control techniques in Table I.

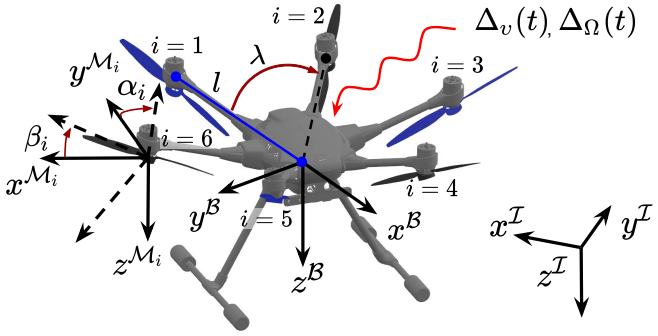

Fig. 1: The Hexa-rotor's coordinate frames $\mathcal{I}$, $\mathcal{B}$, and $\mathcal{M}_i$. Here, all motors are located at a distance l from the center of the UAV and tilted at fixed angles $\beta = -25°$, $\alpha = 35°(-1)^i$ and $\lambda = 60°$. Note that $i = \{1, 2, ..., 6\}$ indexes the $i-$th motor. Disturbances are defined as $\Delta_v(t), \Delta_\Omega(t)$.

B. Contribution

We present a robust position controller for the fully-actuated Hexa-rotor that utilizes a fractional-order integral, as illustrated in Fig. 2. Our proposed control algorithm achieves globally exponential stability of the tracking error equilibrium. Furthermore, it exhibits strong robustness, as demonstrated in the stability proof and realistic software-in-the-loop simulations (SITL). In addition, we have made

[1]G. Flores, A. Montes de Oca, and A. Flores are with the Laboratorio de Percepción y Robótica (LAPyR), Center for Research in Optics, Loma del Bosque 115, León, Guanajuato, 37150 Mexico. gflores@cio.mx, andresmr@cio.mx, alejandrofl@cio.mx

[2]M. Rakotondrabe is with the Laboratoire Génie de Production, National School of Engineering in Tarbes (ENIT), University of Toulouse, Tarbes, France. mrakoton@enit.fr

TABLE I: The relevant state-of-the-art of fully-actuated Hexa-rotor control. GES, LES, and GAS mean globally exponentially stable, locally exponentially stable, and globally asymptotically stable, respectively.

Literature	Consider disturbance	Stability achieved	Code released	Method
Our research	✓	GES in attitude and position	✓	Fractional-order control
[22]	✓	GES in attitude and position	✗	Nonlinear model predictive control
[23]	✓	GES in attitude and position	✗	Feedback linearization
[24]	✓	GAS in attitude and position	✗	Adaptive sliding mode control
[25]	✓	Ultimate boundedness stability	✗	Feedback linearization

a significant effort to contribute to the UAV and control community by providing open-source code for direct implementation in the PX4 firmware. For that aim, we have developed the fractional-order integral in C++ and added it to the PX4 firmware for implementation. The implementation of our proposed fractional-order control surpasses the performance of the current PID control programmed by default in the PX4 firmware, which is currently the most popular open-source autopilot code for various UAVs. Finally, we have compared our controller and the PX4-firmware controller to validate our claim. All the code developed for this paper and its proper documentation is available in our GitHub repository:
https://github.com/andresmr13/Hexarotor_fractional_control_for_PX4.git
This implementation can be tested using the Hexa-rotor model in a virtual environment, as shown in Fig. 3, or even in a real multi-rotor platform.

C. Outline

The remainder of this letter is described next. Section II introduces the problem to be addressed, including preliminaries and the system's mathematical model. Section III presents the theorems and proofs for the proposed control law. Then, in Section IV, the control implementation through numerical simulations is described. In this section, we present the performance results of the proposed control against state-of-the-art controls. Finally, Section V briefly summarizes the results achieved and considerations for future work.

NOMENCLATURE

(α_i, β_i) Tilted angles of the motors w.r.t. $\mathcal{B}$
$\Delta_v(t), \Delta_\Omega(t) \in \mathbb{R}^3$ Exogenous unknown disturbances affecting the position and orientation dynamics, respectively
$\hat{e}_3 = [0,\ 0,\ 1]^\intercal$ Basis vector for z direction
$\mathcal{B}$ Hexa-rotor body frame
$\mathcal{I}$ Hexa-rotor inertial frame
$\mathcal{M}_i$ Body frame of i-th motor, $i = \{1, 2, ..., 6\}$
$\Omega = [\omega_x,\ \omega_y,\ \omega_z]^\intercal \in \mathbb{R}^3$ Hexa-rotor's angular rate
$\mu = [\mu_x,\ \mu_y,\ \mu_z]^\intercal \in \mathbb{R}^3$ Torque vector considered as control input for the position dynamics Σ
g Gravity constant
$J \in \mathbb{R}^{3\times3}$ Hexa-rotor's inertia matrix
m Hexa-rotor mass
$p = [x,\ y, z]^\intercal$ Hexa-rotor's position vector in $\mathcal{I}$
$R \in$ SO(3) Rotation matrix from $\mathcal{B}$ to $\mathcal{I}$ representing the Hexa-rotor's orientation
$u_\tau = [u_{\tau_x},\ u_{\tau_y},\ u_{\tau_z}]^\intercal \in \mathbb{R}^3$ Torque vector considered as control input for the attitude dynamics Π
$v = [\dot{x},\ \dot{y},\ \dot{z}]^\intercal$ Hexa-rotor's velocity vector in $\mathcal{I}$

The *hat* map $\hat{(\cdot)} : \mathbb{R}^3 \to \mathfrak{so}(3)$ is defined by $\hat{a}b = a \times b$, $\forall\ a, b \in \mathbb{R}^3$, and then $\hat{\Omega} \in \mathfrak{so}(3)$ is the skew-symmetric matrix of Ω; the inverse of the hat map is the *vee* map $(\cdot)^\vee : \mathfrak{so}(3) \to \mathbb{R}^3$.

II. PROBLEM FORMULATION

A. Preliminaries

Definition 1 (The Riemann–Liouville fractional differintegral, [26], [27])**.** *Consider the real-valued function $f(x)$. The Riemann-Liouville fractional derivative is defined by,*

$$ {}_aD_x^\alpha f(x) = \frac{1}{\Gamma(n-\alpha)} \frac{d^n}{dx^n} \int_a^x \frac{f(t)}{(x-t)^{\alpha+1-n}} dt \quad (1) $$

where a, x are the lower and upper limits, $n \in \mathbb{N}$, $(n-1 < \alpha < n)$, and $\Gamma(z)$ is the gamma function defined by,

$$ \Gamma(z) = \int_0^\infty \tau^{z-1} e^{-\tau} d\tau. $$

And the Riemann-Liouville fractional integral is defined by,

$$ {}_aD_x^{-\alpha} f(x) = {}_aI_x^\alpha f(x) = \frac{1}{\Gamma(\alpha)} \int_a^x (x-t)^{\alpha-1} f(t) dt. \quad (2) $$

B. Mathematical model

The Hexa-rotor has six fixed tilted motors as shown in Fig. 1, numbered clockwise as $i = 1, 2, 3, 4, 5, 6$. In addition, each motor is tilted at specific angles (α_i, β_i), which determine the orientation of the motor frame $\mathcal{M}_i$ relative to the Hexa-rotor body frame $\mathcal{B}$. The mathematical model in the 6-DOF of the Hexa-rotor is as follows, [28]:

$$ \Sigma : \begin{cases} \dot{p} = v & (3a) \\ \dot{v} = g\hat{e}_3 - \frac{1}{m} R\mu + \Delta_v(t) & (3b) \end{cases} $$

$$ \Pi : \begin{cases} \dot{R} = R\hat{\Omega} & (4a) \\ \dot{\Omega} = -J^{-1}(\Omega \times J\Omega) + J^{-1}u_\tau + \Delta_\Omega(t). & (4b) \end{cases} $$

The structure of the control input vector in (3b) is $\mu = (\mu_1,\ \mu_2,\ \mu_3)^\intercal$, which opens up the possibility of having a component of the total thrust in the $x-y$ plane, even when $R = I_{3\times3}$, i.e. when the aerial robot is in hover flight mode. On the other hand, for conventional Hexa-rotors where all the rotors point upwards, the input control vector has a fixed structure $\mu = (0,\ 0,\ T)^\intercal$, where T is the total thrust.

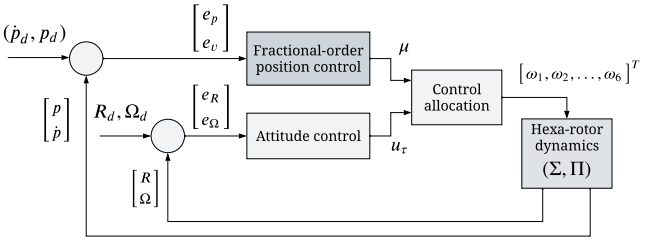

Fig. 2: Block diagram of the proposed fractional-order control.

III. Main Result

To stabilize the fully-actuated Hexa-rotor's dynamics, we must control subsystems Σ and Π, [29]. In our previous work [30], we achieved controlling the attitude subsystem Π. This paper focuses on ameliorating previous work with a powerful controller that rejects aggressive exogenous disturbances. Thus, the proposed controller is separated into the attitude control law to stabilize the error dynamics of subsystem Σ and the fractional-order position controller to stabilize the error dynamics of subsystem Π, which is the core of the contribution.

A. Attitude control

Theorem 1 (Attitude control, [30])**.** *Consider the attitude system Π in* (4)*. And let us define the errors related to attitude dynamics by:*

$$\begin{aligned} e_R &= \frac{1}{2}\big(R_{e,r} - R_{e,r}^\intercal\big)^\vee = [e_R(1),\ e_R(2),\ e_R(3)]^\intercal, \\ e_\Omega &= \Omega - R_{e,r}^\intercal \Omega_d = [e_\Omega(1),\ e_\Omega(2),\ e_\Omega(3)]^\intercal, \\ \Psi_{SO(3)} &= \frac{1}{2}\operatorname{Tr}(I_{3\times 3} - R_{e,r}), \end{aligned} \tag{5}$$

where the right attitude error is $R_{e,r} = R_d^\intercal R$, where R_d is the reference angular position, and $I_{3\times 3}$ is the identity matrix of dimension 3*. Then, the control law*

$$\begin{aligned} u_\tau = -J\,(k_R e_R + k_\Omega e_\Omega + k_3 \upsilon_R + k_4 \upsilon_\Omega) + \Omega \times J\Omega \\ - J(\hat{\Omega} R_{e,r}^\intercal \Omega_d - R_{e,r}^\intercal \dot{\Omega}_d). \end{aligned} \tag{6}$$

with vector signals

$$\upsilon_R = \begin{bmatrix} |e_R(1)|^{1/2} \operatorname{sgn} e_R(1) \\ |e_R(2)|^{1/2} \operatorname{sgn} e_R(2) \\ |e_R(3)|^{1/2} \operatorname{sgn} e_R(3) \end{bmatrix},\ \upsilon_\Omega = \begin{bmatrix} |e_\Omega(1)|^{1/2} \operatorname{sgn} e_\Omega(1) \\ |e_\Omega(2)|^{1/2} \operatorname{sgn} e_\Omega(2) \\ |e_\Omega(3)|^{1/2} \operatorname{sgn} e_\Omega(3) \end{bmatrix} \tag{7}$$

exponentially stabilizes the zero equilibrium points (5)*.*

Proof. The proof of this result can be seen in our previous contribution [30]. □

B. Position control

For the fully-actuated Hexa-rotor position dynamics Σ, we define the error vectors given by,

$$e_p = p - p_d, \qquad e_v = v - \dot{p}_d, \tag{8}$$

where p_d is the desired position trajectory and $(\dot{p}_d, \ddot{p}_d)$ are their the first and second time-derivatives, respectively. They are computed analytically, when possible, or even using advanced differentiator techniques to mitigate the problem of noisy signal derivatives, [31].

Assumption 1. *The external disturbances in system (Σ, Π) are bounded as follows,*

$$\|\Delta_v(t)\|_2 \le \rho_1 \|s\|_2, \qquad \|\Delta_\Omega(t)\|_2 \le \rho_2 \|e_\Omega\|, \tag{9}$$

where s is defined in (13)*, $(\|\cdot\|_2)$ is the Euclidean norm, and $\rho_1, \rho_2 \in \mathbb{R}_{>0}$.*

We are ready to present the main result in the following theorem.

Theorem 2. *Consider that system Σ satisfies Assumption 1. Also consider the fractional-order integral operator I^α defined in* (2)*. Then, the fractional control law,*

$$-\frac{1}{m} R\mu = -K_1 I^\alpha \left(|s|^{\frac{1}{2}} \operatorname{sgn} s \right) - K_2 s - g\hat{e}_3 + \ddot{p}_d - \Lambda e_v \tag{10}$$

and fractional-order differential equation in s,

$$D^{\alpha+1} s = -K_1 \underbrace{\begin{pmatrix} |s_1|^{\frac{1}{2}} \operatorname{sgn} s_1 \\ |s_2|^{\frac{1}{2}} \operatorname{sgn} s_2 \\ |s_3|^{\frac{1}{2}} \operatorname{sgn} s_3 \end{pmatrix}}_{|s|^{\frac{1}{2}} \operatorname{sgn} s} - K_2 D^\alpha \underbrace{\begin{pmatrix} s_1 \\ s_2 \\ s_3 \end{pmatrix}}_{s} \tag{11}$$

where $\alpha \in (0,1)$, $(K_1, K_2, \Lambda) \in \mathbb{R}^{3\times 3} \succ 0$, globally exponentially stabilizes the error equilibrium point (8)*.*

Proof. Let us begin by computing the first-time derivatives of the error vectors in (8) by,

$$\dot{e}_p = e_v, \quad \dot{e}_v = g\hat{e}_3 - \frac{1}{m} R\mu + \Delta_v(t) - \ddot{p}_d. \tag{12}$$

Now, we propose the following sliding surface $s \in \mathbb{R}^3$,

$$s = e_v + \Lambda e_p = [s_1,\ s_2,\ s_3]^\intercal \tag{13}$$

whose time-derivative along the solutions of (12) is:

$$\dot{s} = g\hat{e}_3 - \frac{1}{m} R\mu + \Delta_v(t) - \ddot{p}_d + \Lambda e_v. \tag{14}$$

Now, we are ready to proceed with the stability analysis [32]. Let us consider the candidate Lyapunov function $V = s^\intercal P s$ with $P \succ 0$ whose time-derivative along the solutions of (14) is given by,

$$\begin{aligned} \dot{V} &= \dot{s}^\intercal P s + s^\intercal P \dot{s} \\ &= \left(g\hat{e}_3 - \frac{1}{m} R\mu + \Delta_v(t) - \ddot{p}_d + \Lambda e_v \right)^\intercal P s \\ &\quad + s^\intercal P \left(g\hat{e}_3 - \frac{1}{m} R\mu + \Delta_v(t) - \ddot{p}_d + \Lambda e_v \right). \end{aligned} \tag{15}$$

Notice that when we applied the fractional integral of order α to (11) [33], [34], the result is:

$$\begin{aligned} I^\alpha \Big(D^{\alpha+1} s = -K_1 |s|^{\frac{1}{2}} \operatorname{sgn} s - K_2 D^\alpha s \Big) \\ D^1 s = -K_1 I^\alpha |s|^{\frac{1}{2}} \operatorname{sgn} s - K_2 D^0 s \\ \dot{s} = -K_1 I^\alpha |s|^{\frac{1}{2}} \operatorname{sgn} s - K_2 s. \end{aligned} \tag{16}$$

By equating the previous equation with (14), assuming that the disturbance $\Delta_v(t)$ is unknown, and solving for $-\frac{1}{m}R\mu$, we get the control law defined in (10). We then substitute (10) in (15) to get,

$$\begin{aligned}\dot{V} &= \left(-[I^{\alpha}(|s|^{\frac{1}{2}}\operatorname{sgn} s)]^{\intercal}K_1^{\intercal} - s^{\intercal}K_2^{\intercal} + \Delta_v(t)^{\intercal}\right)Ps \\ &\quad + s^{\intercal}P\left(-K_1[I^{\alpha}(|s|^{\frac{1}{2}}\operatorname{sgn} s)] - K_2 s + \Delta_v(t)\right) \\ &= -[I^{\alpha}(|s|^{\frac{1}{2}}\operatorname{sgn} s)]^{\intercal}K_1^{\intercal}Ps - s^{\intercal}PK_1[I^{\alpha}(|s|^{\frac{1}{2}}\operatorname{sgn} s)] \\ &\quad - s^{\intercal}K_2^{\intercal}Ps - s^{\intercal}PK_2 s + \Delta_v(t)^{\intercal}Ps + s^{\intercal}P\Delta_v(t).\end{aligned} \tag{17}$$

Moreover, notice that

$$\begin{aligned}I^{\alpha}(|s_i|^{\frac{1}{2}}\operatorname{sgn} s_i) &= \frac{1}{\Gamma(\alpha)}\int_0^{s_i}(s_i-\tau)^{\alpha-1}|\tau_i|^{\frac{1}{2}}\operatorname{sgn}\tau_i \mathrm{d}\tau \\ &= \underbrace{\frac{\sqrt{\pi}s_i^{\alpha+\frac{1}{2}}}{2\Gamma\left(\alpha+\frac{3}{2}\right)}}_{b_i}s_i\end{aligned} \tag{18}$$

where $b_i > 0$. Without loss of generality and for the sake of simplicity, we adopt $\alpha = 1/2$ in the subsequent analysis. Then, $I^{\alpha}(|s|^{\frac{1}{2}}\operatorname{sgn} s) = Bs$, where $B = [b_1,\ b_2,\ b_3] \in \mathbb{R}^{3\times 3} \succ 0$. It follows that (17) can be simplified as,

$$\begin{aligned}\dot{V} &= -s^{\intercal}BK_1^{\intercal}Ps - s^{\intercal}PK_1Bs \\ &\quad + s^{\intercal}\left(-K_2^{\intercal}P - PK_2\right)s + 2\Delta_v(t)^{\intercal}Ps.\end{aligned} \tag{19}$$

Since $-K_2$ is negative definite, then $-K_2^{\intercal}P - PK_2 = -Q$, where $Q \succ 0$. Also, consider the first inequality of Assumption 1. Then, it follows that,

$$\dot{V} \leq -s^{\intercal}\underbrace{\left(2BK_1^{\intercal}P + Q - 2\rho_1 P\right)}_{R}s, \tag{20}$$

where we choose $2BK_1^{\intercal}P + Q > 2\rho_1 P$. Furthermore, since

$$\begin{aligned}\lambda_{\min}\{P\}\|s\|_2^2 \leq V \leq \lambda_{\max}\{P\}\|s\|_2^2, \\ -\lambda_{\max}\{R\}\|s\|_2^2 \leq \dot{V} \leq -\lambda_{\min}\{R\}\|s\|_2^2\end{aligned} \tag{21}$$

we conclude that $\dot{V} \leq -\frac{\lambda_{\min}\{R\}}{\lambda_{\max}\{P\}}V$, and since V is radially unbounded it follows that s exponentially converges to zero. This implies that the sliding surface (13) is reduced to $\dot{e}_p = -\Lambda e_p$. Thus, the error equilibrium point (8) is GES. □

IV. Simulations

A. MATLAB Simulink numerical simulations

Simulations with MATLAB Simulink were conducted using different orders of integration α for the proposed fractional-order control. Once a suitable set of parameters was selected for our control, it was compared to a PID control, simulated in MATLAB. Due to space limitations, these simulation appears in the supplementary material, which contains a detailed document describing the simulation results and the MATLAB Simulink files.

B. SITL simulation

In this subsection, we present the implementation of the proposed fractional-order controller in the PX4 firmware through Software in the Loop simulation. These simulations run in a virtual environment in Gazebo, using a 3D model for the fully-actuated Hexa-rotor shown in Fig. 1.

1) Fractional-order integrator computation: Since the PX4 firmware is programmed in C++, any control addition should be developed using the same programming language. However, this is a challenging task mainly due to the complex computation of the fractional-order integral. For this reason, we use Oustaloup's method to obtain a numerical approximation. This method uses conventional transfer functions to represent a band-limited approximation of a fractional-order operator. When attempting to approximate a fractional integrator of order α using a conventional transfer function, it is necessary to calculate the poles and zeros of the transfer function through the use of the following, [35]:

$$\begin{aligned}G_p(\sigma) &= \prod_{k=-N}^{N}\frac{\sigma+\omega_k'}{\sigma+\omega_k}, \\ \omega_k &= \left(\frac{b\omega_h}{d}\right)^{\frac{\alpha+2k}{2N+1}}, \qquad \omega_k' = \left(\frac{d\omega_b}{b}\right)^{\frac{\alpha-2k}{2N+1}},\end{aligned} \tag{22}$$

where N is the order of approximation in the valid frequency range (ω_b, ω_h), with $b,\ d \in \mathbb{R}$ as fixed parameters. The transfer function $G_p(\sigma)$ depends on the frequency domain's complex variable σ.

Thus, to make this process practical, the algorithm is decomposed into two steps: 1) compute the continuous-time transfer function of the fractional-order integral and 2) solve its equivalent state-space equations to get the integrated value. Please refer to Algorithm 1 for an overview of the procedures explained next.

The first step is conducted in MATLAB, and the second is conducted through an integrator block in C++. In MATLAB, we create a zero-pole-gain model with the Oustaloup approximation of the fractional-order integrator I^{α} through (22). Then, the transfer function G_p can be converted to its state-space representation:

$$\dot{x} = Ax + Bu, \quad y = Cx + Du, \tag{23}$$

where, $A \in \mathbb{R}^{n\times n}$, $B \in \mathbb{R}^{n\times 1}$, $C \in \mathbb{R}^{1\times n}$, and $D \in \mathbb{R}$ are constant and strictly depend on the fractional integration order that is being used in the approximation. The input variable u is the signal to be integrated, defined in (13), and the output variable y is the fractional-order integrated signal equivalent to the $I^{\alpha}(u)$. Then, we begin with the second step to compute y from the state-space model through C++ in the PX4 firmware. First, we need to take the state-space matrices (A, B, C, D) as constant parameters for the control algorithm. The process for computing a fractional-order integrated value involves first integrating $\dot{x}$ to obtain x, which is then used to compute y. Once y is obtained, it can be used in the fractional control law (10), substituting the term $I^{\alpha}(|s|^{\frac{1}{2}}\operatorname{sgn} s)$. Finally, solving μ from (10) generates

control input for the UAV system. Besides, when a different fractional order is utilized, repeating the first step from the outset becomes necessary.

Algorithm 1 Computation of fractional-order integral operator for implementation in the PX4 Firmware.

Require: α, s
Ensure: Fractional-order integral y
  Initialize d,b, N, w_b, w_h, k, x, t, t_{prev}, $\dot{x}$, $\dot{x}_{prev}$ with default values.
  $w_{kp} \leftarrow (w_h/w_b)^((k+N+0.5-0.5*\alpha)/(2*N+1)) * w_b$
  $w_k \leftarrow (w_h/w_b)^((k+N+0.5+0.5*\alpha)/(2*N+1)) * w_b$
  $K \leftarrow (d * w_h/b)^\alpha$
  $G_p \leftarrow zpk(-w_{kp'}, -w_{k'}, K) * tf([d, b*w_h, 0], [d*(1-\alpha), b*w_h, d*\alpha])$ ▷ zero-pole-gain form function
  $G \leftarrow tf(G_p)$ ▷ convert to transfer function
  $A, B, C, D \leftarrow tf2ss(G)$ ▷ convert to state-space
  while True **do**
    $u \leftarrow sqrt(|s|) * sgn(s)$ ▷ s from (13)
    $\dot{x} \leftarrow A * x + B * u$
    $y \leftarrow C * x + D * u$ ▷ y is equivalent to $I^\alpha(u)$
    $\Delta t \leftarrow t - t_{prev}$
    $\Delta x \leftarrow (\dot{x} + \dot{x}_{prev}) * \Delta t/2$ ▷ integer-order integration
    $x \leftarrow \Delta x$
    $\dot{x}_{prev} \leftarrow \dot{x}$
    $t_{prev} \leftarrow t$
    $t \leftarrow t + 1$
  end while

2) Results: In the following, we present the results from the software in the loop (SITL) simulation, where the proposed control is programmed into the PX4 firmware and tested in a virtual environment in Gazebo. The fully-actuated Hexa-rotor's virtual model is shown in Fig. 3.

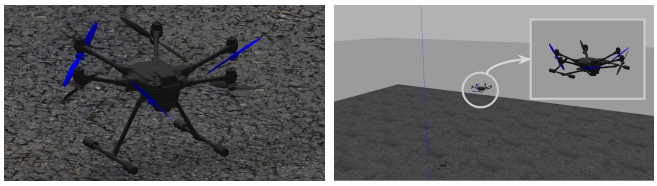

(a) (b)

Fig. 3: a) The fully-actuated Hexa-rotor model in a Gazebo virtual environment. b) Hexa-rotor flying during the SITL experiment.

The simulation consists of a hover flight of the Hexa-rotor in the $x = y = 0$ coordinates, achieving an altitude of 2.5 m from the $x = y = z = 0$ position. An external disturbance of $4\sin(0.5t)$ for the x axis and $3\sin(0.1t)$ for the y axis is applied to verify the position controller's performance. We also compare the performance of our fractional-order position controller and the PID controller, commonly used in UAVs and coded by default in the PX4 firmware. This comparison is shown in Fig. 4. It can be seen that the behavior of the UAV while applying the proposed fractional-order control (black line) is considerably more stable than the

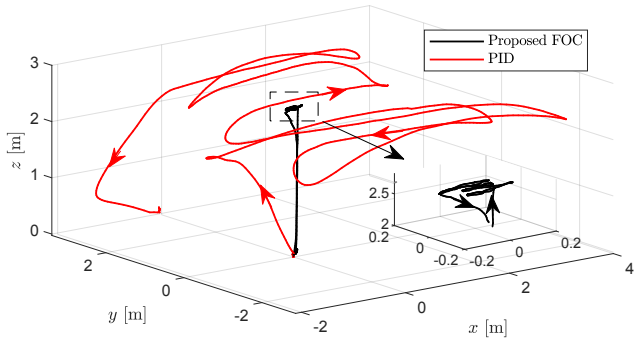

Fig. 4: In SITL simulations, we monitored the position states of the fully-actuated Hexa-rotor. The UAV's position trajectory was visualized with two lines: black for our proposed fractional-order control and red for the standard PID control in PX4 firmware. Analyzing these results provides evidence of our control strategy's advantages.

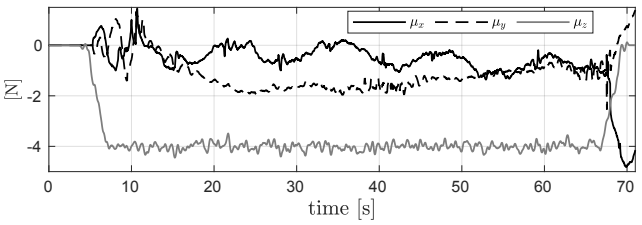

Fig. 5: Fractional-order position control obtained during the SITL simulation of the fully-actuated Hexa-rotor.

position with the PID control (red line). In the case of the proposed control, the error obtained does not exceed the 0.2 m in both axes. On the contrary, the PID control does not provide enough robustness against disturbances, with an error reaching more than 1 m and, in certain moments, even 4 m. Finally, Fig. 5 depicts the control signals obtained during the hovering flight applying the proposed control approach. It is observed that the control inputs are continuous and relatively smooth without any chattering effect.

V. Conclusions

In this research, we have presented the design of a fractional-order control system for the position dynamics of a fully-actuated Hexa-rotor. Our proposed control system is demonstrated to be well-suited for increasing the system's robustness against disturbances. Furthermore, the proposed control law provides global exponential stability to the error equilibrium of the positioning system. Furthermore, we perform MATLAB and software-in-the-loop simulations in a virtual environment using Gazebo to emulate the PX4 firmware in which the control algorithm is programmed. Finally, to demonstrate the superiority of our proposed control system, we also compare it with the performance of the PID control system. Note that PID is the standard controller programmed in the PX4-firmware used for various UAVs worldwide in the drones and robotics communities. The results show that the fractional-order control system is

significantly more robust for the position states of the Hexa-rotor than the standard PX4-firmware controller (the PID).

This work enhances our previous results in this research subject: [30], [36]. We plan to conduct real flight experiments using a fully-actuated Hexa-rotor constructed in the lab.

The implemented PX4 code for this paper is available in our GitHub repository, where the reader can find supplementary material, including additional simulations with their corresponding files.

REFERENCES

[1] M. Lungu, D.-A. Dinu (Vîlcică), M. Chen, and G. Flores, "Inverse optimal control for autonomous carrier landing with disturbances," *Aerospace Science and Technology*, vol. 139, p. 108382, 2023.

[2] G. Flores, "Longitudinal modeling and control for the convertible unmanned aerial vehicle: Theory and experiments," *ISA Transactions*, vol. 122, pp. 312–335, 2022.

[3] R. Cajo, T. T. Mac, D. Plaza, C. Copot, R. De Keyser, and C. Ionescu, "A survey on fractional order control techniques for unmanned aerial and ground vehicles," *IEEE Access*, vol. 7, pp. 66 864–66 878, 2019.

[4] A. Flores and G. Flores, "Implementation of a neural network for nonlinearities estimation in a tail-sitter aircraft," *Journal of Intelligent & Robotic Systems*, vol. 103, no. 22, 2021.

[5] A. M. de Oca and G. Flores, "The AgriQ: A low-cost unmanned aerial system for precision agriculture," *Expert Systems with Applications*, vol. 182, p. 115163, 2021.

[6] A. Montes de Oca and G. Flores, "A uas equipped with a thermal imaging system with temperature calibration for crop water stress index computation," in *2021 International Conference on Unmanned Aircraft Systems (ICUAS)*, 2021, pp. 714–720.

[7] R. Verdín, G. Ramírez, C. Rivera, and G. Flores, "Teleoperated aerial manipulator and its avatar. communication, system's interconnection, and virtual world," in *2021 International Conference on Unmanned Aircraft Systems (ICUAS)*, 2021, pp. 1488–1493.

[8] M. Labbadi and M. Cherkaoui, "Adaptive fractional-order nonsingular fast terminal sliding mode based robust tracking control of quadrotor UAV with gaussian random disturbances and uncertainties," *IEEE Transactions on Aerospace and Electronic Systems*, vol. 57, no. 4, pp. 2265–2277, 2021.

[9] M. Labbadi, Y. Boukal, and M. Cherkaoui, "Path following control of quadrotor UAV with continuous fractional-order super twisting sliding mode," *Journal of Intelligent and Robotic Systems*, vol. 100, 12 2020.

[10] X. Shi, Y. Cheng, C. Yin, S. Zhong, X. Huang, K. Chen, and G. Qiu, "Adaptive fractional-order SMC controller design for unmanned quadrotor helicopter under actuator fault and disturbances," *IEEE Access*, vol. 8, pp. 103 792–103 802, 2020.

[11] C. Hua and J. Chen, "Fractional-order sliding mode control of uncertain QUAVs with time-varying state constraints," *Nonlinear Dynamics*, vol. 95, p. 1347–1360, 01 2019.

[12] C. Izaguirre-Espinosa, A. J. Muñoz-Vazquez, A. Sanchez-Orta, V. Parra-Vega, and I. Fantoni, "Fractional-order control for robust position/yaw tracking of quadrotors with experiments," *IEEE Transactions on Control Systems Technology*, vol. 27, no. 4, pp. 1645–1650, 2019.

[13] M. Vahdanipour and M. Khodabandeh, "Adaptive fractional order sliding mode control for a quadrotor with a varying load," *Aerospace Science and Technology*, vol. 86, pp. 737–747, 2019.

[14] C. Yin, B. Hu, Y. Cheng, J. Xue, and X. Shi, "Design of fractional-order backstepping sliding mode controller for the quadrotor unmanned aerial vehicles," in *2018 37th Chinese Control Conference (CCC)*, 2018, pp. 697–702.

[15] M. Pouzesh and S. Mobayen, "Event-triggered fractional-order sliding mode control technique for stabilization of disturbed quadrotor unmanned aerial vehicles," *Aerospace Science and Technology*, vol. 121, p. 107337, 2022.

[17] R. Ayad, W. Nouibat, M. Zareb, and Y. Bestaoui Sebanne, "Full control of quadrotor aerial robot using fractional-order FOPID," *Iranian Journal of Science and Technology, Transactions of Electrical Engineering*, vol. 43, no. 1, pp. 349–360, Jul 2019.

[16] F. Oliva-Palomo, A. J. Muñoz-Vázquez, A. Sánchez-Orta, V. Parra-Vega, C. Izaguirre-Espinosa, and P. Castillo, "A fractional nonlinear PI-structure control for robust attitude tracking of quadrotors," *IEEE Transactions on Aerospace and Electronic Systems*, vol. 55, no. 6, pp. 2911–2920, 2019.

[18] J. Song, Y. Hu, J. Su, M. Zhao, and S. Ai, "Fractional-order linear active disturbance rejection control design and optimization based improved sparrow search algorithm for quadrotor UAV with system uncertainties and external disturbance," *Drones*, vol. 6, no. 9, p. 229, 2022.

[19] J. Lavín-Delgado, Z. Zamudio Beltrán, J. Gómez-Aguilar, and E. Pérez-Careta, "Controlling a quadrotor UAV by means of a fractional nested saturation control," *Advances in Space Research*, vol. 71, no. 9, pp. 3822–3836, 2022.

[20] Z. Yu, Y. Zhang, B. Jiang, C.-Y. Su, J. Fu, Y. Jin, and T. Chai, "Refined fractional-order fault-tolerant coordinated tracking control of networked fixed-wing UAVs against faults and communication delays via double recurrent perturbation fnns," *IEEE Transactions on Cybernetics*, pp. 1–13, 2022.

[21] Z. Yu, Y. Zhang, B. Jiang, B. Jiang, C.-Y. Su, J. Fu, Y. Jin, and T. Chai, "Nussbaum-based finite-time fractional-order backstepping fault-tolerant flight control of fixed-wing UAV against input saturation with hardware-in-the-loop validation," *Mechanical Systems and Signal Processing*, vol. 153, p. 107406, 2021.

[22] D. Shawky, C. Yao, and K. Janschek, "Nonlinear model predictive control for trajectory tracking of a hexarotor with actively tiltable propellers," in *2021 7th International Conference on Automation, Robotics and Applications (ICARA)*, 2021, pp. 128–134.

[23] G. Michieletto, N. Lissandrini, A. Antonello, R. Antonello, and A. Cenedese, "Dual quaternion delay compensating maneuver regulation for fully actuated UAVs," *IFAC-PapersOnLine*, vol. 53, no. 2, pp. 9316–9321, 2020, 21st IFAC World Congress.

[24] J. M. Arizaga, H. Castaneda, and P. Castillo, "Adaptive control for a tilted-motors hexacopter UAS flying on a perturbed environment," in *2019 International Conference on Unmanned Aircraft Systems (ICUAS)*, 2019, pp. 171–177.

[25] A. Baldini, R. Felicetti, A. Freddi, S. Longhi, and A. Monteriu, "Disturbance observer based fault tolerant control for tilted hexarotors," in *2021 International Conference on Unmanned Aircraft Systems (ICUAS)*, 2021, pp. 20–27.

[26] Y. Chen, I. Petras, and D. Xue, "Fractional order control - a tutorial," in *2009 American Control Conference*, 2009, pp. 1397–1411.

[27] A. Atangana, "Chapter 1 - history of derivatives from Newton to Caputo," in *Derivative with a New Parameter*, A. Atangana, Ed. Academic Press, 2016, pp. 1–24.

[28] G. Flores and R. Lozano, "Lyapunov-based controller using singular perturbation theory: An application on a mini-UAV," in *2013 American Control Conference*, 2013, pp. 1596–1601.

[29] A. Flores, R. Verdín, H. Moreno, and G. Flores, "Development, model, simulation, and real test of a new fully actuated quadrotor," in *2023 International Conference on Unmanned Aircraft Systems (ICUAS)*, 2023, pp. 1324–1330.

[30] G. Flores, A. M. de Oca, and A. Flores, "Robust nonlinear control for the fully actuated hexa-rotor: Theory and experiments," *IEEE Control Systems Letters*, vol. 7, pp. 277–282, 2023.

[31] A. Levant, M. Livne, and X. Yu, "Sliding-mode-based differentiation and its application," *IFAC-PapersOnLine*, vol. 50, no. 1, pp. 1699–1704, 2017, 20th IFAC World Congress.

[32] S. Liu, W. Jiang, X. Li, and X.-F. Zhou, "Lyapunov stability analysis of fractional nonlinear systems," *Applied Mathematics Letters*, vol. 51, pp. 13–19, 2016.

[33] Y. Luchko, "Fractional derivatives and the fundamental theorem of fractional calculus," *Fractional Calculus and Applied Analysis*, vol. 23, no. 4, pp. 939–966, 2020.

[34] I. Podlubny, *Fractional differential equations: an introduction to fractional derivatives, fractional differential equations, to methods of their solution and some of their applications*. San Diego, CA, USA: Academic Press, 1999.

[35] A. Tepljakov, V. Vunder, E. Petlenkov, S. S. Nakshatharan, A. Punning, V. Kaparin, J. Belikov, and A. Aabloo, "Fractional-order modeling and control of ionic polymer-metal composite actuator," *Smart Materials and Structures*, vol. 28, no. 8, p. 084008, jul 2019.

[36] A. Flores and G. Flores, "Fully actuated hexa-rotor UAV: Design, construction, and control. simulation and experimental validation," in *2022 International Conference on Unmanned Aircraft Systems (ICUAS)*, 2022, pp. 1497–1503.